Available online at www.sciencedirect.com

ScienceDirect

Geochimica et Cosmochimica Acta 185 (2016) 182–197

Geochimica et Cosmochimica Acta

www.elsevier.com/locate/gca

Compositional variation within thick (>10 m) flow units of Mauna Kea Volcano cored by the Hawaii Scientific Drilling Project

Shichun Huang [a,*], Michael J. Vollinger [b], Frederick A. Frey [c], J. Michael Rhodes [b], Qun Zhang [d]

[a] Department of Geoscience, University of Nevada, Las Vegas, United States
[b] Department of Geosciences, University of Massachusetts Amherst, United States
[c] Department of Earth, Atmospheric and Planetary Sciences, Massachusetts Institute of Technology, United States
[d] School of Earth and Space Sciences, University of Science and Technology of China, China

Available online 1 February 2016

Abstract

Geochemical analyses of stratigraphic sequences of lava flows are necessary to understand how a volcano works. Typically one sample from each lava flow is collected and studied with the assumption that this sample is representative of the flow composition. This assumption may not be valid. The thickness of flows ranges from <1 to >100 m. Geochemical heterogeneity in thin flows may be created by interaction with the surficial environment whereas magmatic processes occurring during emplacement may create geochemical heterogeneities in thick flows. The Hawaii Scientific Drilling Project (HSDP) cored ~3.3 km of basalt erupted at Mauna Kea Volcano. In order to determine geochemical heterogeneities in a flow, multiple samples from four thick (9.3–98.4 m) HSDP flow units were analyzed for major and trace elements. We found that major element abundances in three submarine flow units are controlled by the varying proportion of olivine, the primary phenocryst phase in these samples. Post-magmatic alteration of a subaerial flow led to loss of SiO_2, CaO, Na_2O, K_2O and P_2O_5, and as a consequence, contents of immobile elements, such as Fe_2O_3 and Al_2O_3, increase. The mobility of SiO_2 is important because Mauna Kea shield lavas divide into two groups that differ in SiO_2 content. Post-magmatic mobility of SiO_2 adds complexity to determining if these groups reflect differences in source or process. The most mobile elements during post-magmatic subaerial and submarine alteration are K and Rb, and Ba, Sr and U were also mobile, but their abundances are not highly correlated with K and Rb. The Ba/Th ratio has been used to document an important role for a plagioclase-rich source component for basalt from the Galapagos, Iceland and Hawaii. Although Ba/Th is anomalously high in Hawaiian basalt, variation in Ba abundance within a single flow shows that it is not a reliable indicator of a deep source component. In contrast, ratios involving elements that are typically immobile, such as La/Nb, La/Th, Nb/Th, Ce/Pb, Sr/Nd, La/Sm, Sm/Yb, Nb/Zr, Nb/Y and La/Yb, are uniform within the units, and they can be used to constrain petrogenetic processes. Nevertheless all elements are mobile under some conditions. For example, a surprising result is that relative to other samples, the uppermost sample collected from subaerial flow Unit 70, less than 1 m below the flow surface, is depleted in P, HREE and Y relative to all other samples from this flow unit. This result is complementary to the P, REE and Y enrichment found in subaerial lava flows from several Hawaiian shields, e.g., Kahoolawe and Koolau Volcanoes. These enrichments require mobilization of REE and followed by deposition a P-rich mineral.

* Corresponding author.
E-mail address: shichun.huang@unlv.edu (S. Huang).

http://dx.doi.org/10.1016/j.gca.2016.01.015
0016-7037/

1. INTRODUCTION

Major objectives of the Hawaii Scientific Drilling Project (HSDP) were to determine the temporal variation in geochemical characteristics of lavas erupted at Mauna Kea Volcano, and to understand the magmatic history of a Hawaiian volcano as it approaches, overrides and recedes from the Hawaiian hotspot (Stolper et al., 1996). Following a 1 km pilot hole, HSDP-1, drilled in 1996 (see papers in Special Session of Hawaii Scientific Drilling Project in J. Geophys. Res. 1996), in 1999 Phase 1 of HSDP-2 cored 3098 m of basalt; the upper 245 m are from Mauna Loa volcano, and lower 2853 m are from Mauna Kea Volcano. Within the Mauna Kea section, 345 flow units were identified (DePaolo et al., 1999; Garcia et al., 2007). Above 1079 mbsl the units are subaerial lava flows, and below this depth the core includes submarine pillow lavas, massive flow units (possibly intrusive) as well as hyaloclastites (DePaolo et al., 1999; Garcia et al., 2007). In 2005, the HSDP hole was deepened and recovered a further 408 m of basaltic lavas (3098–3506 mbsl), including submarine lavas and several dikes (Rhodes et al., 2012). Analyses of these units show significant temporal variations in geochemical characteristics (see papers on Theme of Hawaii Scientific Drilling Project in Gechemistry, Geophysics, Geosystems 2005; Garcia et al., 2007; Blichert-Toft and Albarède, 2009; Rhodes et al., 2012; Nobre Silva et al., 2013).

It is often assumed that a single sample accurately represents the composition of the flow unit. Therefore to characterize the temporal geochemical variations in the drill core, only one or two samples were analyzed for each HSDP flow unit. These samples, the HSDP reference suite, were distributed to many analytical facilities, thereby ensuring that most geochemical analyses were conducted on the same rock powder. However, evaluation of geochemical variations among units requires determining and understanding the geochemical variability within a single unit. The objective of this study is to determine the variability of major and trace element abundances in multiple samples (5–7) from four thick, 9.3 to 98.4 m, flow units.

Previous study of the geochemical variation in a single, thick (11 m), Tertiary tholeiitic basalt flow from Eastern Iceland (Lindstrom and Haskin, 1981) showed that the intra-flow compositional variations exceed the analytical uncertainty, and reflect variation in proportions of phenocrysts, groundmass minerals, and residual melt. Multiple (14) samples from a thick (15 m) highly alkalic, melilite nephelinite flow of the rejuvenated stage Honolulu Volcanics in Oahu, Hawaii were studied by Clague et al. (2016). The intra-flow compositional variations are larger than analytical uncertainty, and they are attributed to variable phenocryst proportions, segregation of pegmatoid veins, and mobility of Na, K, Sr, Ba, Rb, Pb and U in a fluid phase. In contrast, Rhodes (1983) studied lavas from 16 historical eruptions of Mauna Loa volcano in Hawaii, and found that most flows were homogeneous and that the geochemical variations in these lavas primarily reflect variable olivine contents. As another example, the Mauna Loa 1984 eruption has been carefully studied by taking 67 samples over three three-week eruption period from a 20 km long vent system, and their chemical compositions are almost within analytical uncertainty (Rhodes, 1984).

2. SAMPLE SELECTION

It is imperative to distinguish geochemical features that reflect the mantle source of basalt from those that reflect magmatic processes, such as varying extents of melting and crystallization occurring in the mantle and crust. Within the HSDP core, most of the flow units have experienced some postmagmatic alteration (e.g., Fig. 4 of Huang and Frey, 2003). The alteration environment varies with depth: subaerial for the upper most units (245–1079 mbsl, 834 m of core) and submarine for the underlying units (1079–3506 mbsl, 2427 m of core). We chose Unit 70, a 9.3 m thick subaerial pahoehoe flow in the upper part of the core, to determine the effect of subaerial postmagmatic alteration. In the submarine part of the core olivine-rich basalts are abundant and we studied Unit 284, a 49.4 m thick unit, that has abundant glass analyses that can be compared with the whole-rock compositions.

Some Mauna Kea units have compositional and isotopic similarities to tholeiitic basalt from Loihi Seamount. That is lavas with relatively low SiO_2, high Nb/Zr and $^3He/^4He$ and distinctive Pb isotopic ratios. It is well known that shields forming Hawaiian islands define two subparallel spatial trends, known as the Kea- and Loa-trends. Shield lavas on these two trends have different compositional and isotopic characteristics (e.g., Abouchami et al., 2005; Huang et al., 2011; Weis et al., 2011). Since Mauna Kea is a Kea-trend volcano, and Loihi is a Loa-trend volcano, their similarity in Pb and He isotopic compositions is a surprise and one of the most significant results arising from the HSDP (Blichert-Toft et al., 2003; Eisele et al., 2003; Huang and Frey, 2003; Kurz et al., 2004; Rhodes and Vollinger, 2004; Seaman et al., 2004; Stolper et al., 2004; Sharp and Renne, 2005; Garcia et al., 2007; Blichert-Toft and Albarède, 2009; Rhodes et al., 2012; Nobre Silva et al., 2013). We selected submarine Units 292 (31.5 m thick) and 293 (98.4 m thick) to determine the compositional variation within thick units of the Low-SiO_2 Group (Huang and Frey, 2003).

3. ANALYTICAL PROCEDURES

Samples were crushed in a tungsten carbide shatter box at the University of Massachusetts at Amherst using the procedure described by Rhodes and Vollinger (2004). Major element contents (Table 1a) and some trace element abundances (Table 1b) were determined by X-ray fluorescence analysis (XRF) at University of Massachusetts at Amherst following the procedure described in Rhodes (1996) and Rhodes and Vollinger (2004), and other trace element abundances (Table 1c) were determined by ICP-MS at MIT following the procedure described in Huang and Frey (2003). The analytical uncertainty and accuracy, as well as data for USGS standard BHVO-2, are discussed in Huang and Frey (2003) and Rhodes and Vollinger (2004).

In order to evaluate the tungsten contamination resulting from use of a tungsten carbide shatterbox to powder

Table 1a
Major element abundances (wt%) of samples from 4 units in HSDP2 core.[a]

Unit	Sample	Depth (mbsl)	SiO_2	TiO_2	Al_2O_3	Fe_2O_3*	MnO	MgO	CaO	Na_2O	K_2O	P_2O_5	Total	LOI
	Top	372.9												
70	SR0166-1.3	373.8	46.64	2.98	13.83	13.96	0.19	10.14	9.91	1.77	0.13	0.27	99.82	2.16
70	SR0166-6.2	375.4	46.80	2.91	13.43	13.51	0.18	10.05	10.50	1.93	0.13	0.32	99.77	0.45
70	SR0166-6.8	375.5	46.96	2.90	13.48	13.39	0.18	9.95	10.53	1.93	0.13	0.32	99.78	0.46
70	SR0167-1.6	376.9	46.83	3.19	13.88	14.16	0.19	9.17	9.90	1.84	0.17	0.34	99.65	2.09
70[b]	SR0167-5.9	378.4	47.85	3.00	13.46	13.39	0.18	8.94	10.39	2.11	0.22	0.33	99.87	0.23
70	SR0168-2.9	380.4	47.32	3.05	13.49	13.75	0.18	9.11	10.23	1.90	0.16	0.32	99.52	1.00
	Bottom	382.2												
	Top	2086.5												
284	SR0754-11.0	2087.5	46.70	1.83	10.02	12.68	0.17	17.84	8.44	1.46	0.24	0.17	99.55	0.31
284	SR0756-1.0	2094.3	46.90	1.85	10.05	12.79	0.18	17.90	8.48	1.38	0.21	0.17	99.89	0.38
284[b]	SR0756-13.25	2098.7	46.38	1.77	9.69	12.69	0.17	18.91	8.16	1.54	0.21	0.17	99.69	0.00
284	SR0757-17.1	2103.8	46.17	1.70	9.19	12.70	0.17	20.11	7.81	1.26	0.20	0.16	99.47	0.28
284	SR0759-9.2	2112.4	46.01	1.66	9.06	12.84	0.18	20.69	7.73	1.10	0.17	0.15	99.58	0.57
284[b]	SR0762-4.6	2123.8	46.69	1.82	9.98	12.67	0.18	17.93	8.40	1.63	0.25	0.17	99.71	-0.10
284	SR0764-2.3	2133.0	46.51	1.81	9.75	12.73	0.17	18.85	8.06	1.31	0.30	0.16	99.65	1.19
	Bottom	2135.9												
	Top	2327.8												
292	SR0801-17.6	2328.9	47.01	2.35	11.90	13.21	0.18	12.44	10.46	1.54	0.29	0.21	99.58	3.72
292	SR0803-0.0	2331.4	47.48	2.38	12.16	13.10	0.18	12.42	10.13	1.28	0.14	0.22	99.49	4.84
292	SR0806-0.5	2337.1	46.89	2.33	11.90	13.15	0.18	12.41	9.93	1.73	0.38	0.21	99.11	0.98
292	SR0808-8.8	2345.4	47.21	2.30	11.89	13.24	0.18	12.86	9.89	1.56	0.38	0.21	99.72	1.14
292	SR0810-0.8	2350.3	47.07	2.37	12.06	13.31	0.18	12.73	10.27	1.39	0.10	0.22	99.70	4.32
292[b]	SR0814-14.4	2357.1	47.18	2.35	12.03	13.17	0.18	12.60	10.13	1.56	0.10	0.22	99.51	3.71
	Bottom	2359.3												
	Top	2359.3												
293	SR0820-2.8	2374.5	47.14	2.31	11.97	13.23	0.18	12.55	9.68	1.56	0.61	0.21	99.42	3.59
293	SR0820-8.1	2376.1	47.35	2.32	11.76	13.34	0.19	13.39	9.74	1.25	0.08	0.22	99.63	5.18
293	SR0823-10.80	2391.4	47.54	2.39	12.06	13.20	0.18	12.30	10.23	1.38	0.10	0.22	99.60	4.78
293[b]	SR0826-20.6	2414.2	47.37	2.32	11.93	13.14	0.18	12.69	9.92	1.69	0.16	0.22	99.61	4.54
293	SR0829-12.70	2429.5	47.09	2.32	12.01	13.09	0.18	12.23	9.90	1.92	0.51	0.21	99.45	1.60
293	SR0832-2.40	2443.7	47.24	2.36	12.06	13.12	0.18	12.24	10.31	1.74	0.14	0.22	99.61	6.89
293	SR0834-7.50	2455.2	47.58	2.35	11.94	13.34	0.18	12.91	9.72	1.09	0.09	0.22	99.42	1.75
	Bottom	2457.7												

[a] All data are obtained by XRF at Univ. of Mass.; see Rhodes and Vollinger (2004) for discussion of accuracy and precision.
[b] Samples from reference suite (DePaolo et al., 1999).
* Total Fe as Fe_2O_3.

the HSDP samples (Rhodes and Vollinger, 2004), four samples, from each of the Units 70, 284, 292 and 293, were measured for W abundance at University of Science and Technology of China. About 4 g of powder was dissolved in a mixture of concentrated HNO_3 and HF. Then W was purified using a cation column as described in Qin et al. (2007) and W abundance was determined using a ELAN DRC II ICP-MS and a synthetic W standard solution.

4. RESULTS

4.1. Comparison between results from XRF and ICP-MS

Six trace elements, Zr, Rb, Sr, Ba, Y and Nb, were analyzed by both XRF and ICP-MS. Except for Y, both techniques obtained similar abundances for these elements (Fig. 1); however, Y abundances obtained by ICP-MS are ~15% higher than those obtained by XRF. This result is similar to that obtained based on HSDP reference suite samples (Huang and Frey, 2003), and reflects different values used for standard reference materials when constructing calibration curves for ICP-MS and XRF analyses. A future inter-lab calibration of XRF and ICP-MS measurements involving Y standard prepared from Y metal should solve this discrepancy.

4.2. Contamination from WC shatterbox

The procedures used to prepare samples for analysis contaminate the sample (e.g., Hickson and Juras, 1986; Norman et al., 1989; Frey et al., 1991a; Weis et al., 2005; Sertek et al., 2015). The use of tungsten carbide to powder samples is well known to introduce significant amounts of Co, W, Ta and C and in some cases Nb to the sample powder. However there are few measurements of how much ratios such as Nb/Zr and Nb/Ta are changed by use of WC to prepare rock powders. Our W data, 3–9 ppm, (Table 1c) on four samples from HSDP Units 70, 284, 292 and 293 are much higher than in typical Hawaiian lavas (<0.5 ppm; Ireland et al., 2009). Also Nb/Ta ranges from

Table 1b
Tracer element abundances (ppm) of samples from 4 units in HSDP2 core by XRF.[a]

Unit	Sample	Nb	Zr	Y	Sr	Rb	Ga	Zn	Ni	Cr	V	Ba
70	SR0166-1.3	16.0	199	28.8	376	1.4	23	132	269	407	260	189
70	SR0166-6.2	15.8	196	28.9	410	0.6	22	117	248	401	248	128
70	SR0166-6.8	15.8	195	29.0	409	0.4	22	120	252	390	252	141
70	SR0167-1.6	17.2	210	31.7	384	1.2	23	140	225	328	249	238
70[b]	SR0167-5.9	16.4	201	29.6	404	0.6	23	124	201	312	255	145
70	SR0168-2.9	16.7	203	30.3	400	0.8	23	132	213	317	268	186
284	SR0754-11.0	9.5	103	17.7	228	3.8	14	112	983	955	190	61
284	SR0756-1.0	9.6	105	18.0	232	3.3	14	112	972	963	196	58
284[b]	SR0756-13.25	9.5	102	17.5	226	3.5	14	111	992	960	191	57
284	SR0757-17.1	8.8	96	16.6	214	3.0	13	111	1151	997	184	60
284	SR0759-9.2	8.7	94	16.3	210	2.7	13	109	1164	965	178	46
284[b]	SR0762-4.6	9.6	104	17.8	232	3.9	14	112	928	1004	197	62
284	SR0764-2.3	9.4	102	17.4	227	5.7	13	112	963	966	198	107
292	SR0801-17.6	12.2	127	21.7	252	4.8	18	122	469	643	244	105
292	SR0803-0.0	11.7	124	21.4	246	2.2	17	117	455	671	230	135
292	SR0806-0.5	12.7	131	21.9	274	7.0	18	122	459	637	249	108
292	SR0808-8.8	12.5	128	21.7	277	6.6	17	123	501	675	248	99
292	SR0810-0.8	12.0	126	21.6	273	1.0	18	121	471	647	241	91
292[b]	SR0814-14.4	12.2	126	21.6	280	0.5	17	120	458	646	232	69
293	SR0820-2.8	12.1	126	21.4	254	12.3	17	121	448	626	249	168
293	SR0820-8.1	11.6	121	20.9	236	1.0	17	122	517	636	225	117
293	SR0823-10.80	11.9	125	21.6	255	0.9	17	125	485	641	229	146
293[b]	SR0826-20.6	11.7	122	21.0	272	2.6	17	116	458	624	210	118
293	SR0829-12.70	12.5	128	21.5	267	10.1	17	120	440	616	235	135
293	SR0832-2.40	12.4	131	22.3	300	1.6	19	123	462	659	236	113
293	SR0834-7.50	11.2	119	20.6	214	1.4	17	117	522	716	210	93

[a] All data are obtained by XRF at Univ. of Mass.; see Rhodes and Vollinger (2004) for discussion of accuracy and precision.
[b] Samples from reference suite (DePaolo et al., 1999).

10.5 to 15.7 (Huang and Frey, 2003; Rhodes et al., 2012), lower and more variable compared to MORB and OIB (16.7 ± 1.8 and 17.1 ± 2, respectively, Kamber and Collerson, 2000). In contrast, Nb/Zr in HSDP tholeiitic lavas ranges from 0.07 to 0.10, similar to other Kea trend volcanoes, such as Kilauea (e.g., Fig. 13 of Huang and Frey, 2003).

4.3. Unit 70 (372.9–382.2 mbsl)

This unit is a moderately olivine-phyric subaerial pahoehoe flow, and is classified as post-shield stage tholeiitic lava (Huang and Frey, 2003). Six samples including one reference suite sample were analyzed by XRF, and five by ICP-MS (Table 1). The MgO content in these samples ranges from 8.94% to 10.14% (Table 1). They have lower SiO_2 and higher Fe_2O_3 (total Fe) contents than the Low-SiO_2 shield lavas deeper in the core (below 834 mbsl) (Fig. 2). These geochemical characteristics, low Si and high Fe, of post-shield stage lavas, are inferred to reflect melt segregation at higher pressure than shield stage lavas (Frey et al., 1990, 1991a; Huang and Frey, 2003; Rhodes and Vollinger, 2004; Rhodes et al., 2012).

Compared with the trends of the ~140 HSDP reference suite samples, Unit 70 samples form steeper, near vertical trends in plots of SiO_2, Fe_2O_3, P_2O_5 and K_2O vs. MgO (Fig. 2). Such trends are not consistent with liquid lines of descent (e.g., black solid lines in Fig. 2a and b) or HSDP whole rock trends. Unit 70 samples form negative LOI-SiO_2 and positive LOI-Fe_2O_3 trends (see inserts in Fig. 2a and b), implying that the steep trends for Unit 70 samples in Fig. 2 reflect post-magmatic subaerial alteration. Based on criteria used by Huang and Frey (2003) that altered HSDP lavas have $K_2O/P_2O_5 < 1$, all samples from this flow have been affected by substantial post-magmatic alteration; the five samples have $K_2O/P_2O_5 < 0.67$ and $Ba/Rb > 75$ (Fig. 3).

SR166-1.3, with the largest LOI (2.16%) among all Unit 70 samples, has the lowest P_2O_5 content (Fig. 2f; Table 1). It also has the lowest abundances of HREEs and Y (Table 1) and lowest Lu/Hf (0.0626, compared to 0.0636–0.0653 in the other four Unit 70 samples) (Fig. 2f inset). This observation is complementary to the enrichment of Y and REEs in some lavas from Kahoolawe Volcano (Fodor et al., 1989), and Koolau Volcano, Sample 69TAN-2 (Roden et al., 1984; Frey et al., 1994). Clearly, under some subaerial conditions REEs are mobile apparently by transport in a fluid and incorporation into secondary phosphate minerals (Fodor et al., 1989).

The Ni content in Unit 70 samples ranges from 201 ppm to 269 ppm (Table 1), and it is positively correlated with MgO content, with a slope similar to that of the HSDP-2 reference suite samples, reflecting minor olivine control (Fig. 4).

Table 1c
Tracer element abundances (ppm) of samples from 4 units in HSDP2 core by ICP-MS.[a]

Unit	Sample	Sc	Rb	Sr	Y	Zr	Nb	Ba	La	Ce	Pr	Nd	Sm	Eu	Gd	Tb	Dy	Ho
70	SR0166-1.3	29.2	2.06	350	31.1	189	16.1	156	14.3	35.1	5.37	25.3	6.66	2.30	7.02	1.11	6.04	1.12
70	SR0166-6.8	29.2	1.14	391	31.7	188	16.3	118	14.2	35.2	5.37	25.5	6.74	2.37	6.99	1.11	6.03	1.11
70	SR0167-1.6	30.1	1.92	367	35.6	203	17.6	208	15.8	37.3	5.86	27.5	7.37	2.49	7.71	1.22	6.65	1.25
70[b]	SR0167-5.9	29.3	1.38	375	32.8	193	16.5	137	14.8	37.4	5.67	26.2	7.13	2.31	7.27	1.14	6.31	1.20
70	SR0168-2.9	30.8	1.42	380	33.4	196	17.0	157	14.9	35.8	5.53	26.7	7.05	2.42	7.33	1.14	6.24	1.16
284	SR0754-11.0	22.4	4.02	224	19.8	100	9.6	67.2	8.02	19.9	2.97	13.9	3.62	1.26	4.06	0.644	3.67	0.72
284	SR0756-1.0	26.0	3.85	244	21.5	107	10.5	66.3	8.56	21.5	3.17	15.0	3.96	1.40	4.32	0.697	3.99	0.77
284[b]	SR0756-13.25	24.3	3.83	225	19.6	101	9.6	61.9	7.64	19.3	2.95	13.7	3.67	1.23	3.94	0.646	3.64	0.70
284	SR0757-17.1	23.2	3.39	215	19.0	95.6	9.2	63.2	7.54	18.6	2.80	13.0	3.46	1.19	3.76	0.619	3.45	0.66
284	SR0759-9.2	22.2	2.88	207	18.4	90.8	8.9	49.9	7.33	18.1	2.71	12.6	3.39	1.16	3.63	0.589	3.33	0.65
284[b]	SR0762-4.6	22.9	3.86	221	19.3	98.3	9.5	64.3	7.95	19.3	2.99	14.0	3.64	1.24	3.88	0.634	3.54	0.71
284	SR0764-2.3	22.7	5.28	214	19.0	96.0	9.2	87.3	7.81	19.0	2.84	13.3	3.56	1.26	3.84	0.622	3.56	0.69
292	SR0801-17.6	27.5	5.09	251	24.5	126	12.6	87.4	9.84	24.4	3.66	17.1	4.58	1.57	4.93	0.791	4.51	0.87
292	SR0803-0.0	28.0	2.44	243	24.7	123	12.6	109	9.71	24.1	3.60	17.1	4.52	1.55	4.84	0.777	4.50	0.87
292	SR0806-0.5	26.7	7.29	269	25.0	126	12.8	101	10.2	25.1	3.81	17.4	4.70	1.64	5.09	0.817	4.59	0.88
292	SR0808-8.8	27.3	6.71	271	24.3	123	12.6	91.9	9.92	24.3	3.65	17.1	4.59	1.60	4.96	0.815	4.51	0.87
292	SR0810-0.8	27.1	1.37	267	24.2	123	12.4	70.6	9.78	24.1	3.61	17.0	4.45	1.56	4.88	0.795	4.40	0.86
292[b]	SR0814-14.4	26.4	1.24	262	23.2	123	12.0	63.5	9.58	23.6	3.65	17.2	4.59	1.55	4.87	0.802	4.31	0.87
293	SR0820-2.8	27.5	12.5	252	24.4	126	12.6	137	9.80	24.1	3.62	17.1	4.47	1.54	4.98	0.788	4.52	0.86
293	SR0820-8.1	25.4	1.46	226	22.9	116	11.8	95.5	9.35	23.0	3.43	16.0	4.28	1.49	4.64	0.751	4.26	0.81
293	SR0823-10.80	26.8	1.58	248	24.0	122	12.3	97.1	9.66	23.8	3.58	16.6	4.47	1.52	4.80	0.788	4.40	0.85
293[b]	SR0826-20.6	27.6	3.07	256	23.2	122	12.0	103	9.38	23.8	3.63	16.7	4.44	1.50	4.69	0.767	4.39	0.84
293	SR0829-12.70	22.9	10.0	267	24.5	126	12.7	113	9.90	24.3	3.69	17.2	4.57	1.59	4.96	0.799	4.52	0.87
293	SR0832-2.40	28.3	2.34	292	25.1	129	12.8	96.5	9.93	24.6	3.72	17.5	4.63	1.59	5.00	0.815	4.50	0.89
293	SR0834-7.50	26.1	1.51	211	23.5	119	11.9	77.5	9.37	23.1	3.49	16.6	4.46	1.55	4.78	0.771	4.39	0.84
	BHVO-2, $n = 4$	30.7	9.13	374	27.1	165	18.2	131	14.8	37.0	5.36	23.8	6.07	2.05	6.09	0.933	5.26	0.98

Unit	Sample	Er	Tm	Yb	Lu	Hf	Ta	Pb	Th	U	W
70	SR0166-1.3	2.80	0.383	2.17	0.300	4.80	1.07	1.07	1.12	0.280	
70	SR0166-6.8	2.82	0.386	2.19	0.308	4.77	1.09	1.04	1.10	0.223	
70	SR0167-1.6	3.14	0.422	2.38	0.339	5.20	1.16	1.22	1.23	0.511	
70[b]	SR0167-5.9	2.90	0.393	2.33	0.323	5.07	1.16	1.18	1.14	0.260	
70	SR0168-2.9	2.90	0.384	2.27	0.320	4.94	1.13	1.04	1.15	0.239	4.4
284	SR0754-11.0	1.84	0.253	1.51	0.213	2.60	0.81	0.67	0.61	0.191	
284	SR0756-1.0	1.95	0.272	1.56	0.221	2.81	0.87	0.69	0.65	0.212	
284[b]	SR0756-13.25	1.75	0.251	1.46	0.218	2.49	0.77	0.66	0.59	0.184	
284	SR0757-17.1	1.73	0.241	1.41	0.197	2.45	0.76	0.61	0.58	0.189	
284	SR0759-9.2	1.67	0.236	1.38	0.202	2.35	0.69	0.59	0.55	0.183	8.9
284[b]	SR0762-4.6	1.77	0.251	1.51	0.207	2.53	0.78	0.69	0.62	0.180	
284	SR0764-2.3	1.80	0.249	1.43	0.206	2.52	0.74	0.62	0.59	0.196	
292	SR0801-17.6	2.21	0.314	1.78	0.250	3.19	0.88	0.80	0.77	0.238	
292	SR0803-0.0	2.22	0.307	1.76	0.251	3.22	0.82	0.80	0.74	0.289	3.2
292	SR0806-0.5	2.27	0.303	1.83	0.257	3.33	1.01	0.84	0.77	0.234	
292	SR0808-8.8	2.26	0.304	1.80	0.255	3.25	1.03	0.81	0.77	0.239	
292	SR0810-0.8	2.17	0.304	1.79	0.250	3.17	0.84	0.79	0.75	0.281	
292[b]	SR0814-14.4	2.20	0.309	1.77	0.253	3.24	0.84	0.81	0.79	0.304	
293	SR0820-2.8	2.20	0.307	1.79	0.245	3.19	0.95	0.80	0.75	0.256	
293	SR0820-8.1	2.11	0.287	1.68	0.235	3.01	0.78	0.75	0.71	0.279	
293	SR0823-10.80	2.17	0.305	1.76	0.242	3.12	0.83	0.78	0.74	0.248	
293[b]	SR0826-20.6	2.09	0.334	1.72	0.244	3.14	0.80	0.86	0.73	0.276	
293	SR0829-12.70	2.27	0.304	1.80	0.257	3.20	1.00	0.81	0.76	0.237	8.9
293	SR0832-2.40	2.30	0.316	1.84	0.264	3.24	0.90	0.81	0.79	0.311	
293	SR0834-7.50	2.23	0.297	1.75	0.247	3.12	0.81	0.76	0.73	0.245	
	BHVO-2, $n = 4$	2.51	0.341	1.97	0.277	4.29	1.22	1.10	1.27	0.431	

[a] All data are obtained by ICP-MS at Mass. Inst. of Tech.; see Huang and Frey (2003) for discussion of accuracy and precision.
[b] Samples from reference suite (DePaolo et al., 1999).

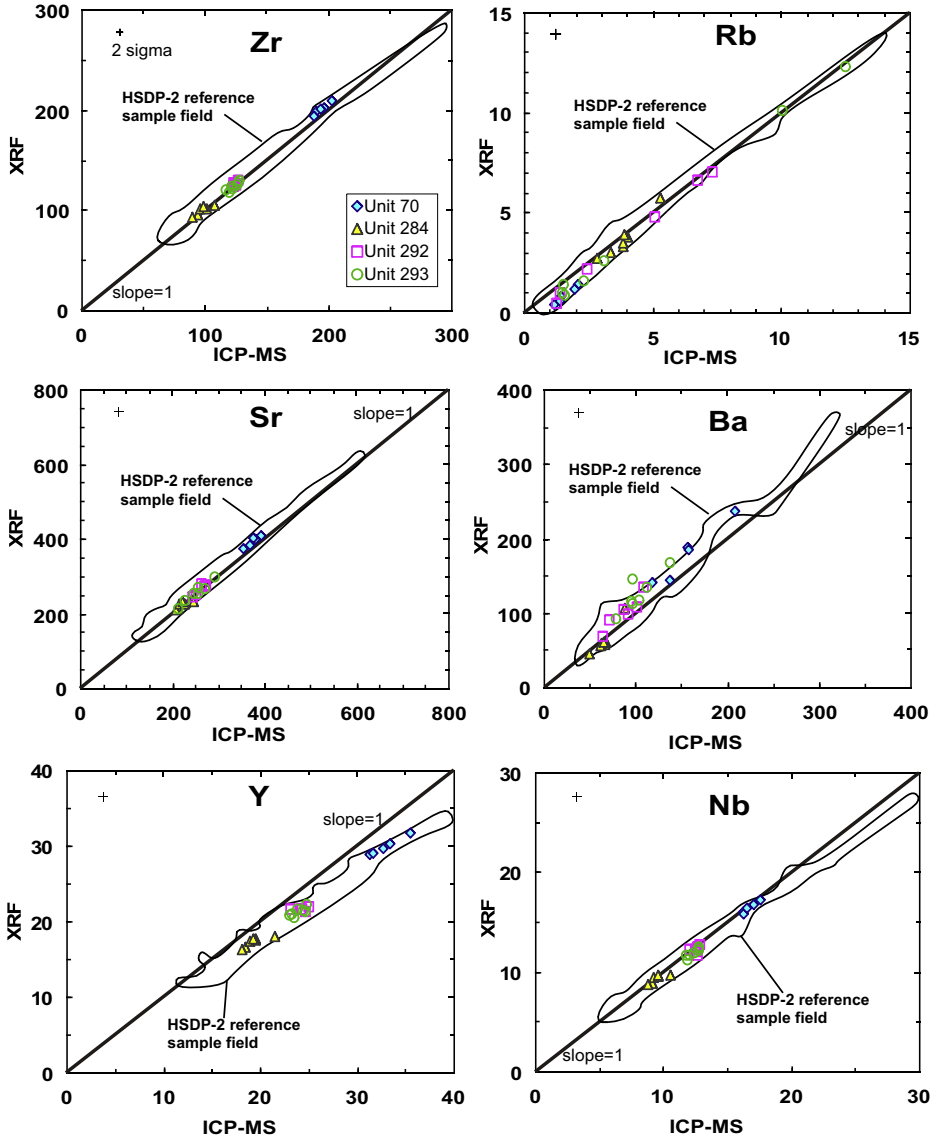

Fig. 1. Comparison of trace element abundances obtained by ICP-MS and XRF. The HSDP-2 reference sample field is from Huang and Frey (2003) and Rhodes and Vollinger (2004). Based on multiple analyses of BHVO-2, the two standard deviation uncertainties are indicated in the upper left of each panel.

Abundances of relatively non-mobile incompatible elements, such as Th, Nb, La, Ce, Pb, Zr, Hf and Ti, are positively correlated with each other (Fig. 5). Within each unit, their abundances range is less than a factor of 1.2 (Table 1, Fig. 6a). In contrast, abundances of K, Rb and U are not correlated with Th abundance (Fig. 5); K, Rb and U are commonly mobile during post-magmatic alteration of Hawaiian lavas (e.g., Lipman et al., 1990; Kennedy et al., 1991; Yang et al., 1996), and their abundances range widely, factors of 2.3 for U, 1.8 for Rb, 1.7 for K (Table 1, Fig. 6a). Ba abundances are correlated with Th abundances in most HSDP samples. In the Unit 70 flow, however, Ba forms a steep trend with Th, intersecting the Th axis (Fig. 5f), that is unlikely to be a magmatic trend.

4.4. Unit 284 (2086.5–2135.9 mbsl)

This is a highly olivine-phyric pillow unit and data are available for seven samples (Table 1). Whole-rock samples from this unit are close to the lower boundary of the High SiO_2 shield stage field in Fig. 2a; however, based on Pb and He isotopic ratios, this unit is classified as a Low SiO_2 shield stage tholeiitic lava (Huang and Frey, 2003). This depth interval (1950–2230 mbsl), in fact, represents a transition from high SiO_2 to low SiO_2 compositions (Fig. 7 of Huang and Frey, 2003; Fig. 20 of Stolper et al., 2004). The compositions and isotopic signatures of HSDP lavas are correlated, and differ in the two SiO_2 groups of shield stage Mauna Kea lavas; however in detail, the geochemical and isotopic boundaries between these two SiO_2 groups are

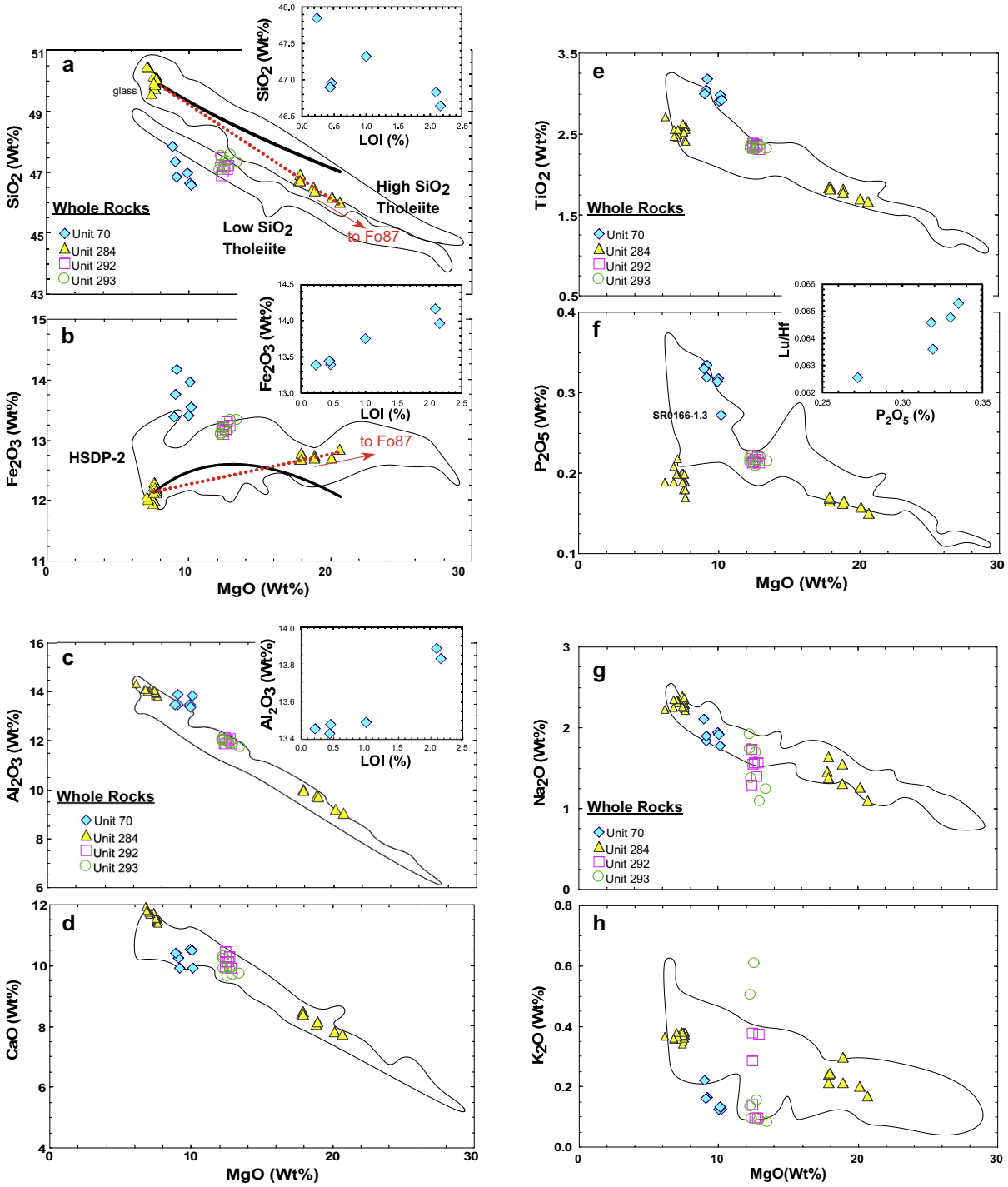

Fig. 2. MgO vs SiO_2, Fe_2O_3, Al_2O_3, CaO, TiO_2, P_2O_5, Na_2O and K_2O (in wt%) in multiple samples from four units. Panels a, b and c have insets for LOI vs SiO_2, Fe_2O_3 and Al_2O_3, respectively and Panel f has an inset for Lu/Hf vs P_2O_5 for Unit 70 samples. Whole rock HSDP-2 reference sample fields are from Rhodes and Vollinger (2004). Note in Panel a that two distinct fields are defined for SiO_2. In all panels, glasses from Unit 284 are plotted (yellow triangles with MgO around 8 wt%; Stolper et al., 2004). Analytical uncertainties are smaller than the symbols. In Panels a and b the black lines show calculated trends for olivine fractionation from a high MgO parental melt to the Unit 284 glasses. The red dotted lines show the calculated trends for olivine accumulation in Unit 284 glasses. For olivine fractionation trends, equilibrium olivine was subtracted from a high MgO melt in steps of 0.5 wt% with $Kd_{Fe/Mg}^{OL/melt} = 0.32$. The high MgO melt composition was chosen so that the olivine fractionation trend intersects the field for Unit 284 glass composition. For the olivine accumulation trends, Fo_{87} olivine was added to the average glass composition. Unit 284 glasses and whole rocks can be related by olivine accumulation, but not by olivine fractionation. (For interpretation of the references to color in this figure legend, the reader is referred to the web version of this article.)

not always consistent. This reflects the fact that isotopic signatures are not affected by partial melting process, but SiO_2 content is controlled by both source composition and extent and pressure of partial melting.

The MgO content in seven Unit 284 whole rock samples ranges from 17.84% to 20.69% (Table 1). Glasses from this unit (Stolper et al., 2004) cluster around MgO of 7.5% (Fig. 2). The whole rocks have CaO/Al_2O_3 of 0.84 ± 0.01 (1σ), and glasses have CaO/Al_2O_3 of 0.83 ± 0.01 (1σ), implying that olivine was the only dominant crystal phase. The geochemical difference between whole rock samples and glasses from this unit can be best explained as a result of accumulating Fo_{87} olivine (Fig. 2a and b). That is, the whole rock samples are mixtures of melt, now glass, and variable amounts of olivine with an average composition of Fo_{87}. In contrast, the glass compositions and whole rock compositions cannot be related to each other via a fractional crystallization process. The black solid lines in Fig. 2a and b indicates the path of melts resulting from fractional crystallization of a high MgO melt, whose composition was selected so that the olivine fractionation trend passes through the Unit 284 glass compositions. However these trends do not pass through the whole rock compositions.

Other major element and Ni contents are highly correlated with MgO content, with slopes similar to those defined by HSDP reference suite samples (Figs. 2 and 4). The abundances of relatively immobile incompatible elements, such as Th, Nb, La, Zr and Pb, are positively correlated (Fig. 5). In contrast, in plots of Th vs Ba, K and Rb, these seven Unit 284 samples form nearly vertical trends (Fig. 5f–h).

Except for SR764-2.3, Unit 284 samples have K_2O/P_2O_5 of 1.26–1.45 and Ba/Rb of 16.2–18.7; these samples are relatively unaltered (Fig. 3). Sample SR764-2.3 with anomalously high K_2O/P_2O_5 (1.82 in Fig. 3) also has anomalously high K, Rb and Ba contents (Fig. 5f–h).

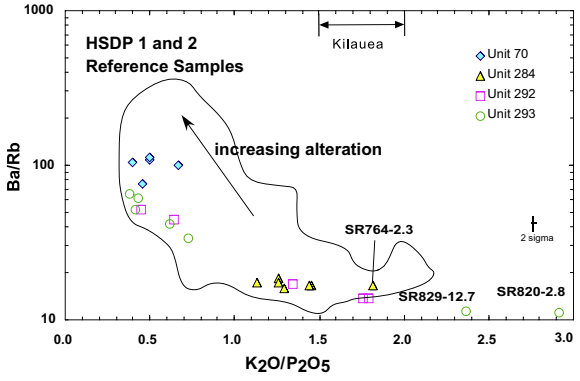

Fig. 3. K_2O/P_2O_5 vs Ba/Rb for multiple samples from Units 70, 284, 292 and 293 compared to field for HSDP reference samples. It is well established that subaerial alteration of Hawaiian shield lavas creates a trend to relatively low K_2O/P_2O_5 and high Ba/Rb. In the HSDP core both subaerial and submarine lavas define this trend (see Fig. 4 of Huang and Frey, 2003). Unaltered oceanic basalt has $Ba/Rb = 11.6 \pm 0.2$ (Hofmann and White, 1983). Samples with anomalously high K_2O/P_2O_5 (>1.7) are labeled. K_2O/P_2O_5 range in fresh Kilauea lavas (Greene et al., 2013) is shown for comparison. Data from this paper, Rhodes (1996), Huang and Frey (2003) and Rhodes and Vollinger (2004).

4.5. Unit 292 (2327.8–2359.3 mbsl)

This unit is a 31.5 m thick aphyric to sparsely olivine-phyric pillow lava, and data are available for six samples (Table 1). The reference suite sample (SR814-14.4) is a typical low SiO_2 shield stage tholeiitic lava (Huang and Frey, 2003).

The MgO content in six samples from this unit varies only from 12.4% to 12.9% (Table 1). Unit 292 samples form a small field in Fig. 2a–f. Consequently, they do not form obvious trends in most panels in Fig. 2; except for plots of MgO vs Na_2O and K_2O where these six samples form vertical trends. These samples are especially useful in assessing the effects of alteration because they range widely in K_2O/P_2O_5 (0.44–1.76) and Ba/Rb (13.7–51.6) over a narrow MgO content (Fig. 3). Although abundances of mobile

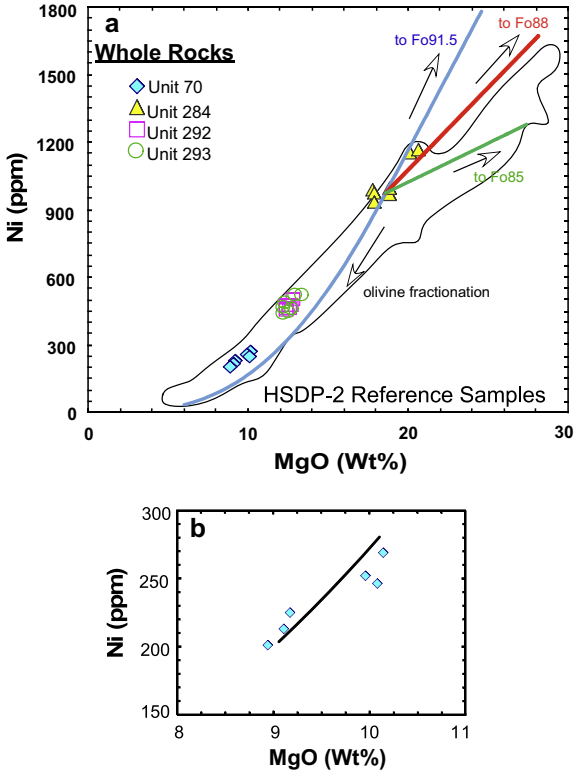

Fig. 4. (a) MgO (wt%) vs Ni (ppm). HSDP reference sample field is from Rhodes and Vollinger (2004). Analytical uncertainties are smaller than the symbols. Model trends of olivine fractionation and accumulation are shown for comparison. In detail, Sample SR641, which Putirka et al. (2011) argued to represent the parental magma for HSDP lavas, was used as the starting composition. For olivine fractionation, equilibrium olivine was removed in steps of 0.5 wt%. $Kd_{Fe/Mg}^{OL/melt} = 0.32$, and $D_{Ni}^{OL/melt} = 3.346*D_{Mg}^{OL/melt} - 3.665$ (Beattie et al., 1991) are used. For olivine accumulation, three olivine compositions were used: $Fo_{91.5}$, the highest olivine Fo found at Mauna Kea (e.g., Baker et al., 1996; Putirka et al., 2011); Fo_{88}, the average HSDP olivine composition (Baker et al., 1996); and Fo_{85}. The MgO–Ni trend of HSDP whole rock lavas may represent olivine fractionation and accumulation. Panel b shows five Unit 70 samples with an olivine fractionation trend that shows the MgO–Ni trend of Unit 70 samples is consistent with olivine fractionation.

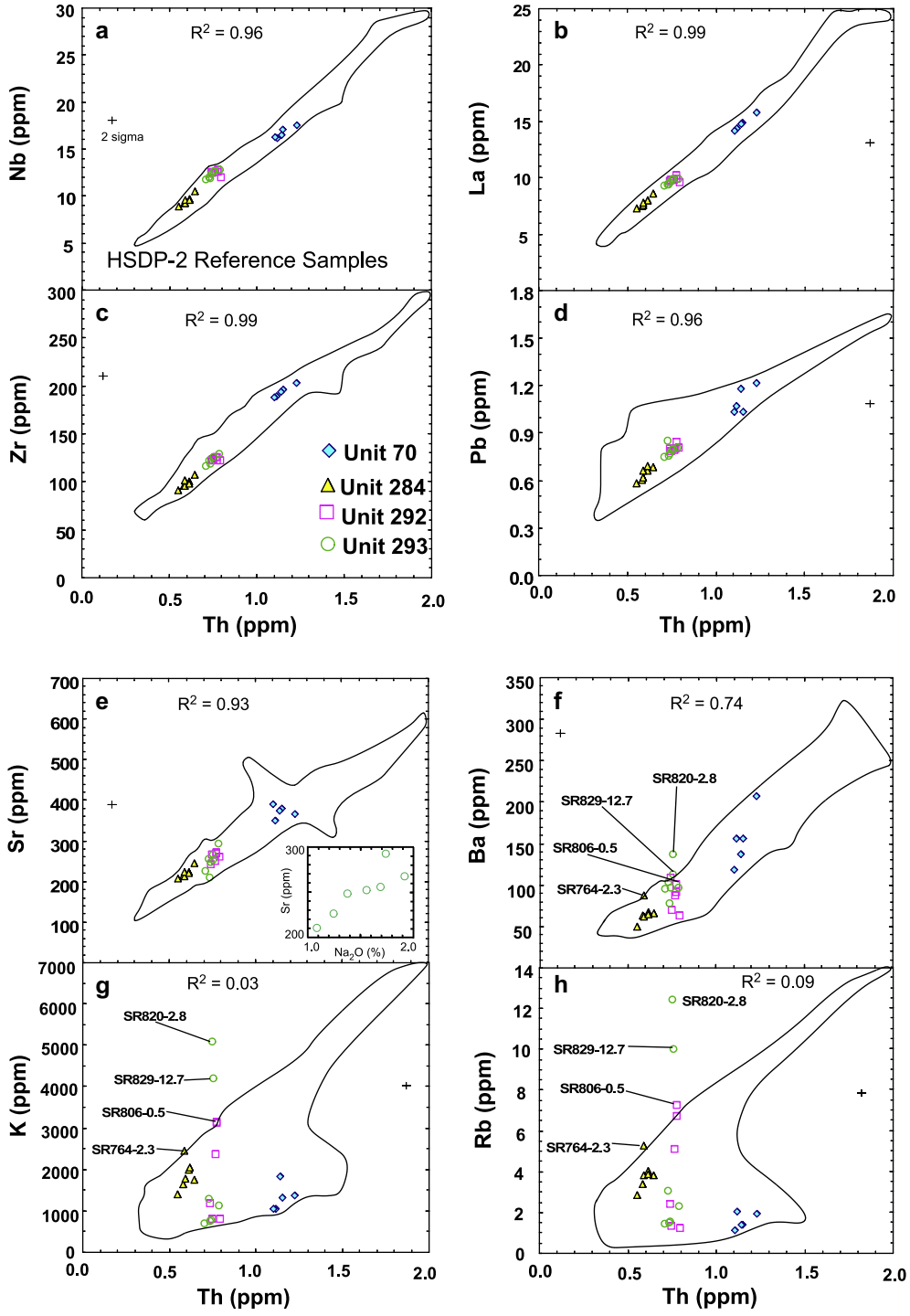

Fig. 5. Th vs Nb, La, Zr, Pb, Sr, Ba, K and Rb (ppm). Samples with anomalous enrichments of K, Rb and Ba are labeled. HSDP-2 reference sample fields are from Huang and Frey (2003) and Rhodes and Vollinger (2004). Two HSDP-2 reference suite samples, SR3465-5.6 and SR531-4.4, with anomalously high Pb abundances are not included in panel d. Panel e shows an inset for Sr vs Na_2O in Unit 293 samples.

elements, such as Ba, Rb and K are highly variable, the six samples have similar non-mobile trace element abundances (Table 1; Figs. 2 and 5), confirming the generally accepted conclusion that abundances of Ti, Nb, Zr, and Th are not commonly changed by postmagmatic alteration; consequently they are referred to as non-mobile elements.

4.6. Unit 293 (2359.3–2457.7 mbsl)

This unit is a very thick (98.4 m) aphyric to sparsely olivine-phyric pillow lava, and seven samples were analyzed (Table 1). The reference suite sample (SR826-20.6) is a typical Low SiO_2 shield stage tholeiitic lava (Huang and Frey,

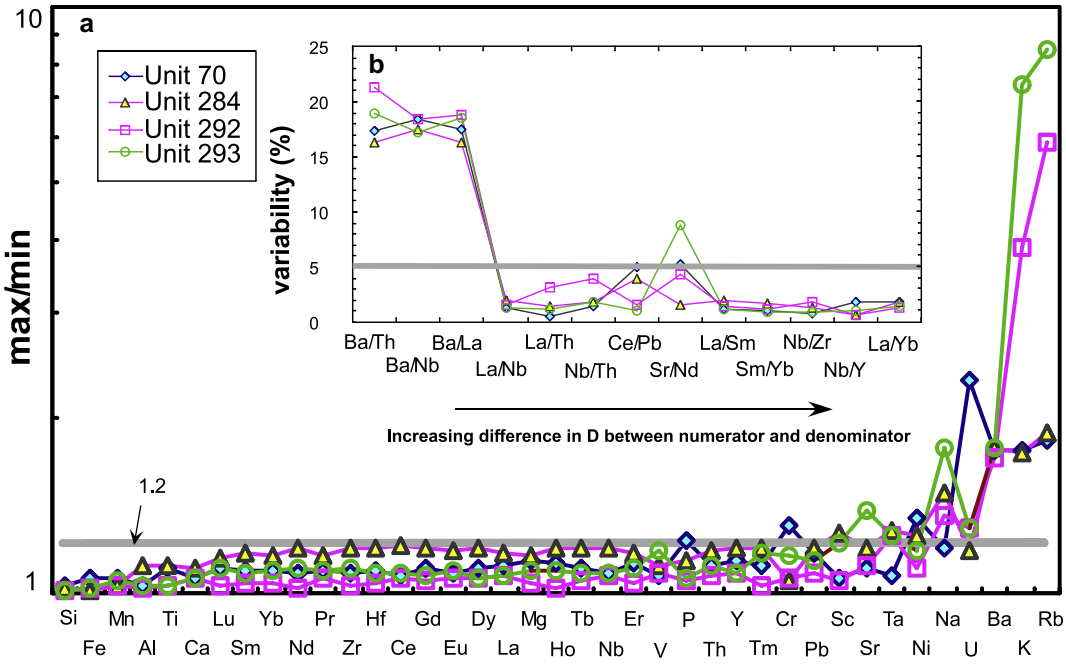

Fig. 6. (a) Element abundance ranges in the four multi-sampled units. An element abundance range in a unit is defined as the ratio of the maximum and minimum element abundances. Ordering of elements is determined by increasing range from left to right; most element ranges are less than 1.2. (b) Variability [(one standard deviation/mean × 100)] in abundance ratios of incompatible elements in Units 70, 284, 292 and 293. Element abundance ratios are ordered based on the difference in D (partition coefficient, from Hofmann, 1988) between numerator and denominator. The maximum analytical uncertainty of element abundance ratios by ICP-MS at MIT is 5% (1-sigma, see appendix of Huang and Frey, 2003). The variability of most incompatible element abundance ratios is less than 5%; however, element abundance ratios involving Ba are highly variable. Also, the Sr/Nd variability in Unit 293 is ~9%, implying moderate Sr mobility.

2003). The MgO content in six samples from this Unit varies only from 12.2% to 13.4% (Table 1). Seven Unit 293 samples have similar immobile major and trace element abundances (Table 1; Figs. 2, 4 and 5). Samples from Units 292 to 293 overlap in a small field in Fig. 2a–f.

As with Unit 292 the seven samples from this unit range widely in K_2O/P_2O_5 and Ba/Rb; however, K_2O/P_2O_5 ratios are grouped with two unusually high values that exceed values for all other HSDP samples (2.4 and 2.9) because of high K_2O content, and five samples having $K_2O/P_2O_5 < 0.73$ and Ba/Rb > 33 (Fig. 3). Also abundances of mobile elements, such as Na_2O, Ba, K_2O and Rb, are highly variable (Table 1; Figs. 2 and 5). Specifically, the ranges of Rb and K_2O in these seven samples are almost as large as that in the whole HSDP reference suite samples (Fig. 5h). The seven Unit 293 lavas form a near vertical trend in plot of Th vs Sr (Fig. 5e), and they also form a positive Na_2O vs. Sr trend (inset in Fig. 5e). Correlated Na and Sr enrichments are also reported for sea water altered MORB (e.g., Fig. 6 of Staudigel et al., 1996). Na enrichment may be caused by Na-bearing secondary phases, such as analcite and natrolite, but these minerals are not enriched in Sr (e.g., Staudigel et al., 1986). Consequently, Staudigel et al. (1996) concluded that the correlated enrichments of Na and Sr cannot be explained by the addition or removal of a single secondary phase. Zeolites, as a secondary mineral, with up to 3.9% SrO and 2.1% Na_2O, have been found in altered Koolau lavas (Weinstein et al., 2004). Sample SR829-12.70 has N_2O of 1.92% and Sr of 267 ppm, so that it is unlikely that the positive Na_2O–Sr trend of Unit 293 samples is controlled by zeolites.

5. DISCUSSION

5.1. Post magmatic processes that change the major element composition of basalt

After eruption, the compositions of oceanic basalt are modified by interaction with fresh water during subaerial alteration, and with seawater during submarine alteration. These water–rock reactions lead to formation of secondary minerals in an open system and results in compositional variability within flows. In the HSDP drill core alteration of hyaloclastites involves dissolution of glassy margins, and formation of secondary minerals, such as smectite and palagonite (Walton and Schiffman, 2003; Walton et al., 2005). During this process some elements, such as alkali metals and alkaline earths, were readily leached from glass and fine-grained groundmass. Compositional heterogeneity in thick flows can also result from deuteric and hydrothermal processes.

Subaerial alteration of Hawaiian lavas usually leads to loss of Si, Mg, Ca, Na, K, Sr, Rb and Ba (e.g., Feigenson et al., 1983; Yang et al., 1996; Huang and Frey, 2003; Révillon et al., 2007), and may also lead to an increase in Fe and Al content as other major elements, such as Si,

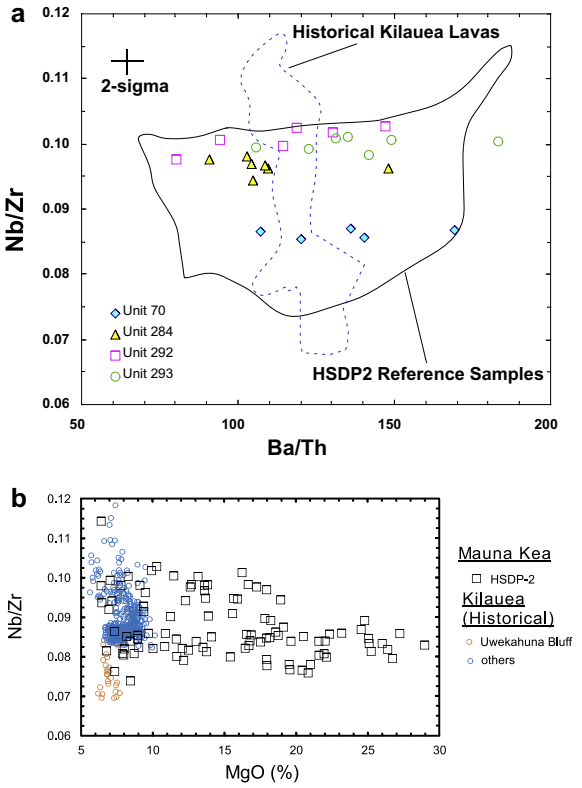

Fig. 7. (a) Ba/Th vs Nb/Zr for multiple samples from Units 70, 284, 292 and 293 compared to data for HSDP reference samples (Huang and Frey, 2003). Note that Ba/Th is much more variable than Nb/Zr, factors of 2.7 and 1.6, respectively. The 2-sigma analytical uncertainty is estimated following Huang and Frey (2003). The field for historical Kilauea lavas (Pietruszka and Garcia, 1999; Marske et al., 2007, 2008; Greene et al., 2013; Pietruszka et al., 2013) shows that within the last 210 years of Kilauea volcanism the Nb/Zr variation has exceeded that found over the 550,000 years of Mauna Kea volcanism represented in the HSDP core. In contrast the range of Ba/Th ratios in historical unaltered Kilauea lavas is much less than in the variably altered Mauna Kea lavas. (b) MgO (%) vs Nb/Zr for HSDP Mauna Kea and historical Kilauea lavas. The large Nb/Zr variation at a given MgO content within Kilauea lavas implies that Nb/Zr was not controlled by crystal fractionation. Specifically, Uwekahuna Bluff Kilauea lavas have the lowest Nb/Zr ratio, and they also have lower $^{206}Pb/^{204}Pb$ and higher $^{87}Sr/^{86}Sr$ than other historical Kilauea lavas (Marske et al., 2007); therefore Nb/Zr is a source signature.

Mg, Ca, Na and K, are leached from the rock (Lipman et al., 1990; Révillon et al., 2007). In contrast, during low temperature submarine alteration where basalts react with seawater, uptake of Si, Al, Mg, K, Na, Rb, Sr, Cs, Ba and U has been observed (e.g., Hart, 1969; Seyfried and Bischoff, 1979; Hart and Staudigel, 1982; Staudigel et al., 1996; Alt, 2003a,b; Walton and Schiffman, 2003; Schramm et al., 2005; Walton et al., 2005). However, during submarine hydrothermal alteration at high temperature (>150 °C) or in a reducing environment, K and Rb are leached away from basalts (e.g., Seyfried and Bischoff, 1979; Thompson, 1984; Frey et al., 1991b).

5.2. Post magmatic processes that created within flow heterogeneity in abundance of major elements in thick HSDP flows

Samples from Units 70 to 284 have relatively large MgO ranges, 8.94–10.14% and 17.84–20.69%, respectively (Table 1, Fig. 2). K_2O/P_2O_5 in six of seven Unit 284 samples ranges from 1.26 to 1.45, but sample SR764-2.3 has K_2O/P_2O_5 of 1.82, and Ba/Rb in these seven samples ranges from 16.2 to 18.7 (Fig. 3); they are unaltered. In Fig. 2, Unit 284 samples form trends with slopes similar to that defined by HSDP reference samples, and these trends extrapolate to the field of Unit 284 glasses, implying that variation of major element contents in Unit 284 is mainly controlled by varying proportions of olivine phenocrysts.

In contrast, Unit 70 samples form steeper trends that that defined by HSDP-2 reference samples in plots of MgO vs SiO_2, Fe_2O_3, P_2O_5, but not Al_2O_3, CaO and TiO_2, with the implication that these major element oxides have not been significantly affected by alteration (Fig. 2). The Unit 70 samples have $K_2O/P_2O_5 < 0.67$ and $Ba/Rb > 75$ (Fig. 4); consequently, we infer that these steep trends are result of both varying proportions of olivine phenocrysts and extent of alteration.

The negative LOI-SiO_2 trend of Unit 70 lavas reflects leaching of SiO_2 during subaerial alteration. The positive LOI-Fe_2O_3 trend might imply that Fe was immobile after being oxidized to Fe^{3+} during subaerial alteration; consequently, its concentration increases as a result of mobile elements, such as SiO_2, Na_2O and K_2O, being leached away (e.g., Révillon et al., 2007). Consistent with this interpretation, within Unit 70, concentrations of other immobile elements, such as Ti_2O and Al_2O_3, are also positively correlated with LOI (Table 1; inset in Fig. 2c), and Unit 70 samples have nearly constant Fe_2O_3/Al_2O_3 of 1.01 $\pm$ 0.01 (1σ). Therefore, within Unit 70, we infer that the negatively correlation of SiO_2 and Fe_2O_3 reflects alteration. Negatively correlated SiO_2–Fe_2O_3 can also be interpreted to reflect varying pressures during partial melting (e.g., Langmuir et al., 1992). Consequently it is important to distinguish between the effects of alteration and magmatic processes.

Leaching of SiO_2 is also observed in subaerial lavas from both Mauna Kea and Mauna Loa Volcanoes (Fig. 9). Specifically, after correction for the effect of olivine fractionation or accumulation, subaerial Mauna Kea and Mauna Loa lavas show positive K_2O/P_2O_5 vs. SiO_2 trends. The SiO_2 differences at a given K_2O/P_2O_5 between Loa and Kea-trend lavas and between the two SiO_2 groups forming the Mauna Kea shield (Fig. 9) are robust with respect to K mobility. These differences in SiO_2 content may reflect different source compositions or different melting processes (Frey and Rhodes, 1993).

5.3. Post magmatic processes that created within flow heterogeneity in abundance of trace elements (plus K, Na and Ti) in thick HSDP flows

Analyses of five to seven samples from each of four flow units in the HSDP core show that abundance of Th, Nb,

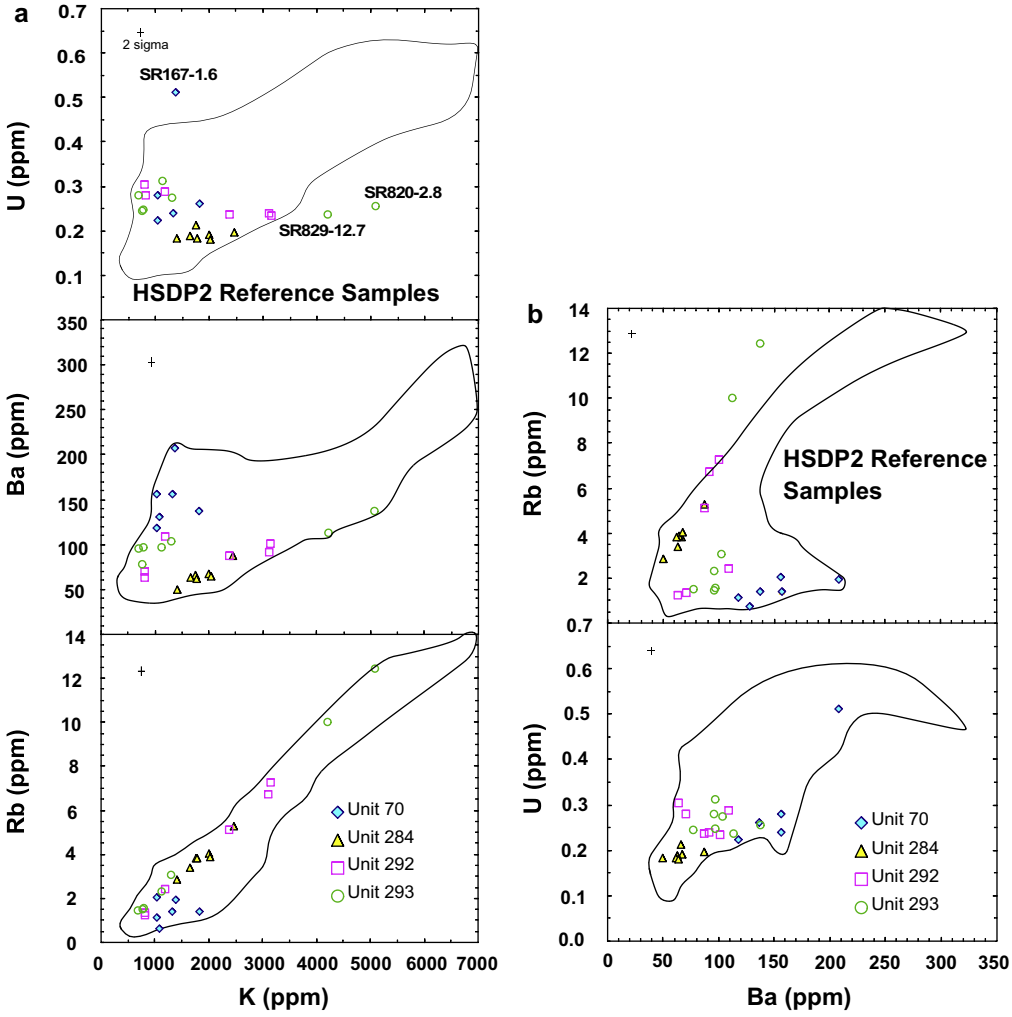

Fig. 8. (a) K vs U, Ba and Rb and (b) Ba vs Rb and U (ppm) for multiple samples from units 70, 284, 292 and 293. These elements are mobile during post-magmatic alteration. Shown for comparison is field for HSDP reference lava suite (Huang and Frey, 2003; Rhodes and Vollinger, 2004).

La, Ce, Pb, Zr, Hf and Ti in each unit varies by <20% (Fig. 6a). Except for Pb, this result is consistent with other studies that found that these elements are immobile during post-magmatic alteration. (e.g., Lindstrom and Haskin, 1981; Rhodes, 1983; Lipman et al., 1990; Pearce, 1996). The uniformity of Pb abundances is also indicated by the limited range of Ce/Pb ratio in these 25 samples, 31 ± 3 (2σ), similar to the average Ce/Pb in MORB (25 ± 1, 2σ) (Gale et al., 2013). This is a surprising result since altered whole-rock sample from Hawaii such as Detroit Seamount in the Emperor Chain, range widely in Ce/Pb (5–65), compared to nearly constant Ce/Pb ratio (31 ± 6, 2σ) in glasses recovered from the same location (Fig. 7 of Huang et al., 2005a). Similarly, Ce/Pb in altered whole rock samples from Kahoolawe, Hawaii ranges from 12 to 29 (Huang et al., 2005b).

The largest compositional variations are in the olivine-phyric Unit 284; the abundance variations of the incompatible elements reflect varying proportions of olivine phenocrysts as reflected by the large range in MgO content, from 17.8% to 20.7% in whole rocks to 7.1% to 7.7% in glasses (Fig. 2). Abundance ratios involving Th, Nb, La, Ce, Pb, Zr, Hf and Ti are quite uniform within each unit (e.g., Fig. 6b); hence a ratio such as Nb/Zr is a useful discriminant that reflects the magmatic processes (Fig. 7; Rhodes et al., 2012). A surprising result is that historical Kilauea lavas, erupted in last ~210 years, vary more in Nb/Zr than the 550,000 years of Mauna Kea volcanism in the HSDP core. The large Nb/Zr variation in Kilauea lavas is likely to be source related because the Uwekahuna Bluff lavas from Kilauea Volcano that define the lower Nb/Zr end of the Kilauea field (Fig. 7b) are also isotopically distinct from other Kilauea lavas (Marske et al., 2007). In contrast, the Ba/Th ratio which involves two highly incompatible elements (in the absence of phlogopite and feldspar) is highly variable within a unit (Fig. 7a). Consequently, we conclude that, unlike Nb/Zr, whole rock Ba/Th should not be used to constrain magmatic processes. Nevertheless high Ba/Th and Sr/Nd ratios, greater than the primitive mantle value, in Hawaiian lavas have been used to argue for recycled plagioclase-rich gabbroic crust, in the Hawaiian plume (Hofmann and Jochum, 1996; Sobolev et al., 2000).

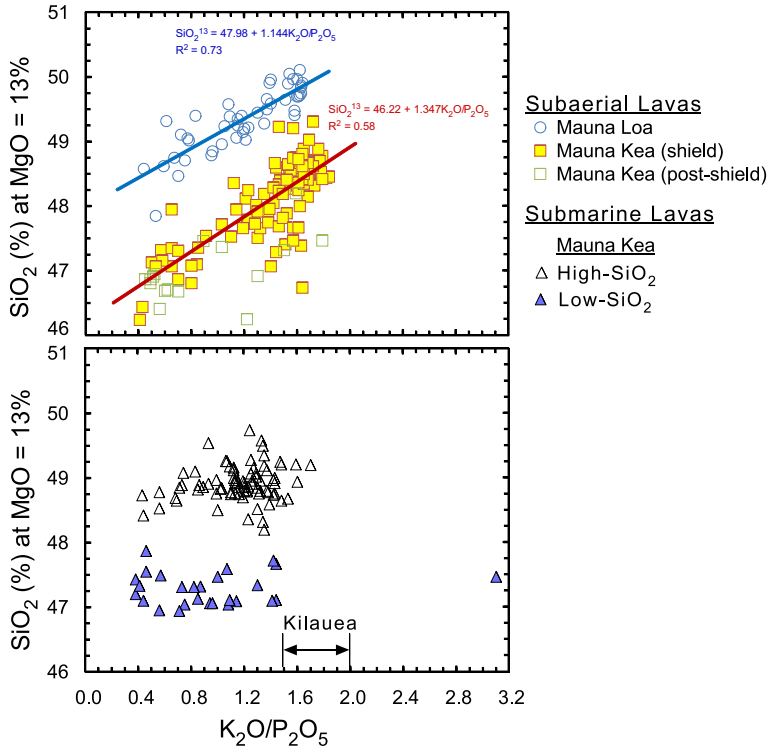

Fig. 9. K_2O/P_2O_5 vs SiO_2^{13} (wt%) for Mauna Loa and Mauna Kea lavas. In order to remove the effects of olivine fractionation or accumulation, SiO_2^{13} content which represents SiO_2 content at MgO of 13 wt% is plotted (see Rhodes and Vollinger, 2004 for details). K_2O/P_2O_5 range in fresh Kilauea lavas (Greene et al., 2013) is shown for comparison. In the upper panel, subaerial shield lavas from Mauna Loa and Mauna Kea define distinct fields with Mauna Loa lavas offset to higher SiO_2. Subaerial lavas show positive K_2O/P_2O_5 vs SiO_2^{13} trends, reflecting K_2O mobility. Although submarine Mauna Kea lavas can be divided into two SiO_2 groups, the SiO_2 content of submarine lavas is not correlated with K_2O/P_2O_5 (the lower panel).

High Ba/Th ratios are also reported for some Icelandic basalts (Chauvel and Hémond, 2000) and Galapagos basalts (Saal et al., 2007), and in both locations the high Ba/Th ratios are attributed to a plagioclase-rich gabbro component in the source. However the correlation between Ba/Th and Sr/Nd in Hawaiian shield lavas is poor (Frey et al., this issue; Pietruszka et al., 2013) and all Hawaiian shield lavas have Ba/Th greater than primitive mantle; hence, it is likely that these two ratios were controlled by different processes (see Frey et al., this issue for a detailed discussion).

Although there is no doubt that the abundance of Na, K, Rb, Ba, and to a lesser extent Sr and U, have been affected by post-magmatic processes (Figs. 2g and h, 5e–h, 7a and 8), there are complex relationships among these elements. For example, K and Rb abundance are strongly positively correlated (Fig. 8a), but the correlation between abundances of Ba and K is complex (Fig. 8a): in subaerial Unit 70 the trend is to relatively high Ba with only modest increases in K and Rb; in Unit 284 Ba is well correlated with K and Rb; in contrast in Units 292 and 293 the most altered samples are markedly enriched in K and Rb with only modest increase in Ba and no increase in U.

These complexities reflect alteration reactions such as interaction of glass and minerals with both fresh and seawater under different temperatures at oxidizing or reducing environments that lead to formation of secondary minerals and leaching of elements, especially from glass and fine-grained groundmass. Low temperature, subaerial alteration of Hawaiian shield lavas typically results in K and Rb loss (e.g., Feigenson et al., 1983; Yang et al., 1996). Behaviors of K and Rb during submarine alteration are more complicated: low temperature submarine alteration of MORB typically increases K and Rb abundance, but submarine alteration under high temperature (>150 °C) or at a reducing environment also lead to loss of K and Rb (e.g., Seyfried and Bischoff, 1979; Thompson, 1984; Frey et al., 1991b; Staudigel et al., 1996). Based on Fig. 3 some of the Phase 2 core has lost K and Rb during alteration, but a few samples, such as SR820-2.8 and SR829-12.70 from Unit 293 have gained K and Rb (Figs. 3 and 9).

6. WHAT HAS BEEN LEARNED BY ANALYSIS OF MULTIPLE SAMPLES FROM FOUR THICK FLOW UNITS IN MAUNA KEA VOLCANO

(1) Analyses of multiple samples, five to seven, from thick HSDP lava flow units show that compositional variations were controlled by subaerial and submarine post magmatic processes as well as varying mixing proportions of olivine phenocrysts and melt.

(2) K and Rb were the most mobile elements during post-magmatic alteration. Typically K and Rb were lost, but there are a few examples of K and Rb gain. Ba and to lesser extents Sr and U were also mobile but their abundances are not highly correlated with K and Rb abundance.
(3) Heterogeneous distribution of P-HREE-Y is observed in subaerial Unit 70. Specifically, Sample SR166-1.3, within 1 m of the upper contact of this lava unit, has lower P_2O_5 and HREE-Y contents, and a lower Lu/Hf ratio. REE-Y enrichment caused by the growth of a secondary phosphate phase; rhabdophane has been reported for subaerial lavas from Kahoolawe Volcano (Fodor et al., 1989). If some samples are enriched in REE and Y as a result of their mobility and subsequent incorporation into a groundmass phosphate, nearby samples, such as SR166-1.3, must be depleted in REE and Y.
(4) Element ratios such as Nb/Zr, La/Nb and Ce/Pb, but not Ba/Th, are uniform (±4%) within a flow unit and are useful indicators of petrogenesis. Usually, Pb is mobile during submarine alteration, leading to variable Ce/Pb in altered submarine lavas (e.g., Fig. 7 of Huang et al., 2005a). However, such Pb mobility is not observed in our studied samples that include some highly altered lavas (with LOI up to 7%). The 25 analyzed lavas have nearly constant Ce/Pb ratio of 31 ± 3 (2σ).
(5) Classification of HSDP basalt based on He and Pb isotopic compositions, may differ from that based on major element composition. For example Unit 284 was classified as a Low-SiO_2 shield lava (Huang and Frey, 2003). However, two reference suite samples from this unit, SR756-13.25 and SR762-4.6, have major element compositions similar to the High-SiO_2 shield group. The high SiO_2 signature of this unit has been confirmed by analyses of five more samples from this unit, implying that the geochemical and isotopic boundaries between two HSDP-2 SiO_2 groups are not always consistent. This is because elemental compositions, such as SiO2 content and Nb/Zr, of a melt are controlled by both source heterogeneity and partial melting process.

ACKNOWLEDGEMENTS

We thank D. DePaolo, E. Stolper and D. Thomas for their leadership of the HSDP, M. Garcia, C. Seaman and the logging crew for their on site efforts, and our colleagues studying these cores. We thank B. Grant for assistance in ICP-MS analysis and P. Dawson for assistance in XRF analysis. We thank M. Baker for discussion. Constructive reviews from R. V. Fodor, and two anonymous reviewers, as well as Guest Editor R. Hickey-Vargas, are highly appreciated. S.H. acknowledges support from NSF awards EAR-1524387 and EAR-1144727.

REFERENCES

Abouchami W., Hofmann A. W., Galer S. J. G., Frey F. A., Eisele J. and Feigenson M. (2005) Lead isotopes reveal bilateral asymmetry and vertical continuity in the Hawaiian mantle plume. *Nature* **434**, 851–856. http://dx.doi.org/10.1038/nature03402.

Alt J. C. (2003a) Alteration of the upper oceanic crust: mineralogy, chemistry and processes. In *Hydrogeology of the Oceanic Lithosphere* (eds. H. Elderfield and E. Davis). Cambridge Univ. Press, New York, pp. 495–533.

Alt J. C. (2003b) Hydrothermal fluxes at mid-ocean ridges and on ridge flanks. *C. R. Acad. Sci. Geosci.* **335**, 853–864.

Baker M. B., Alves S. and Stolper E. M. (1996) Petrography and petrology of the Hawaii Scientific Drilling Project lavas: inferences from olivine phenocryst abundances and compositions. *J. Geophys. Res.* **101**, 11715–11727.

Beattie P., Ford C. and Russell D. (1991) Partition coefficients for olivine-melt and orthopyroxene-melt systems. *Contrib. Mineral. Petrol.* **109**, 212–224.

Blichert-Toft J. and Albarède F. (2009) Mixing of isotopic heterogeneities in the Mauna Kea plume Conduit. *Earth Planet. Sci. Lett.* **282**, 190–200. http://dx.doi.org/10.1016/j.epsl.2009.03.015.

Blichert-Toft J., Weis D., Maerschalk C., Agranier A. and Albarède F. (2003) Hawaiian hot spot dynamics as inferred from the Hf and Pb isotope evolution of Mauna Kea volcano. *Geochem. Geophys. Geosyst.* **4**(2), 8704. http://dx.doi.org/10.1029/2002GC000340.

Chauvel C. and Hémond C. (2000) Melting of a complete section of recycled oceanic crust: trace element and Pb isotopic evidence from Iceland. *Geochem. Geophys. Geosyst.* **1**. http://dx.doi.org/10.1029/1999GC000002.

Clague D. A., Frey F. A., Garcia M. O., Huang S., McWilliams M. and Beeson M. H. (2016) Compositional heterogeneity of the Sugarloaf melilite nephelinite flow, Honolulu Volcanics, Hawai'i. *Geochim. Cosmochim. Acta.* **185,** 251–277.

DePaolo D. J., Stolper E. M., Thomas D. M. and Garcia M. O. (1999) Hawaii Scientific Drilling Project: core logs and summarizing data [CD-ROM].

Eisele J., Abouchami W., Galer S. J. G. and Hofmann A. W. (2003) The 320 kyr Pb isotope evolution of Mauna Kea lavas recorded in the HSDP-2 drill core. *Geochem. Geophys. Geosyst.* **4**(5), 8710. http://dx.doi.org/10.1029/2002GC000339.

Feigenson M. D., Hofmann A. W. and Spera F. J. (1983) Case studies on the origin of basalt. II. The transition from tholeiitic to alkalic volcanism on Kohala volcano, Hawaii. *Contrib. Mineral. Petrol.* **84**, 390–405.

Fodor R. V., Malta D. P., Bauer G. R. and Jacobs R. S. (1989) Microbeam analyses of rare-earth element phosphate in basalt from Kahoolawe Island, Hawaii. In *Proceedings of the 24th Annual Conf* (ed. P. E. Russell). Microbeam Analyt Soc, San Francisco Press, San Francisco, pp. 554–558.

Frey F. A. and Rhodes J. M. (1993) Intershield geochemical differences among Hawaiian volcanoes: implications for source compositions, melting process, and magma ascent paths. *Philos. Trans. R. Soc. Lond. A* **342**, 121–136.

Frey F. A., Wise W. S., Garcia M. O., West H., Kwon S.-T. and Kennedy A. (1990) Evolution of Mauna Kea Volcano, Hawaii: petrologic and geochemical constrains on postshield volcanism. *J. Geophys. Res.* **95**, 1271–1300.

Frey F. A., Garcia M. O., Wise W. S., Kennedy A., Gurriet P. and Albarède F. (1991a) The evolution of Mauna Kea Volcano, Hawaii: petrogenesis of tholeiitic and alkalic basalts. *J. Geophys. Res.* **96**, 14347–14375.

Frey F. A., Jones W. B., Davis H. and Weis D. (1991b) Geochemical and petrological data for basalts from Site 756, 757, and 758: implications for the origin and evolution of Ninetyeast Ridge. In *Proc. ODP, Sci. Results*, 121 (eds. J. Weissel, J. Peirce, E. Taylor,

J. Alt, et al.). College Station, TX (Ocean Drilling Program). pp. 611–659.

Frey F. A., Huang S. and Xu G. (this issue) Plagioclase and clinopyroxene cumulate in the source of hawaiian shield basalt: evidence based on abundance ratios of incompatible elements. *Geochim. Cosmochim. Acta*.

Gale A., Dalton C. A., Langmuir C. H., Su Y. and Schilling J.-G. (2013) The mean composition of ocean ridge basalts. *Geochem. Geophys. Geosyst.* **14**, 489–518. http://dx.doi.org/10.1029/2012GC004334.

Garcia M. O., Haskins E. H., Stolper E. M. and Baker M. (2007) Stratigraphy of the Hawai'i Scientific Drilling Project core (HSDP2): anatomy of a Hawaiian shield volcano. *Geochem. Geophys. Geosyst.* **8**, Q02G20. http://dx.doi.org/10.1029/2006GC001379.

Greene A. R., Garcia M. O., Pietruszka A. J., Weis D., Marske J. P., Vollinger M. J. and Eiler J. (2013) Temporal geochemical variations in lavas from Kilauea's Pu'u O'o eruption (1983–2010): cyclic variations from melting of source heterogeneities. *Geochem. Geophys. Geosyst.* **14**, 4849–4873. http://dx.doi.org/10.1002/ggge.20285.

Hart S. R. (1969) K, Rb, Cs contents and K/Rb, K/Cs ratios of fresh and altered submarine basalts. *Earth Planet. Sci. Lett.* **6**, 295–303.

Hart S. R. and Staudigel H. (1982) The control of alkalies and uranium in seawater by ocean crust alteration. *Earth Planet. Sci. Lett.* **58**, 202–212.

Hickson C. J. and Juras S. J. (1986) Sample contamination by grinding. *Can. Mineral.* **24**, 585–589.

Hofmann A. W. (1988) Chemical differentiation of the Earth: the relationship between mantle, continental crust, and oceanic crust. *Earth Planet. Sci. Lett.* **90**, 297–314.

Hofmann A. W. and Jochum K. P. (1996) Source characteristics derived from very incompatible trace elements in Mauna Loa and Mauna Kea basalts (Hawaiian Scientific Drilling Project). *J. Geophys. Res.* **101**, 11831–11839.

Hofmann A. W. and White W. M. (1983) Ba, Rb and Cs in the Earth's mantle. *Z. Naturforssch.* **38a**, 258–266.

Huang S. and Frey F. A. (2003) Trace element abundances of Mauna Kea basalt from Phase 2 of the Hawaiian Scientific Drilling Project: petrogenetic implications of correlations with major element content and isotopic ratios. *Geochem. Geophys. Geosyst.* **4**(6), 8711, 1029/2002 GC000322, 2003.

Huang S., Regelous M., Thordarson T. and Frey F. A. (2005a) Petrogenesis of lavas from Detroit Seamount: geochemical differences between Emperor Chain and Hawaiian volcanoes. *Geochem. Geophys. Geosyst.* **6**, Q01L06. http://dx.doi.org/10.1029/2004GC000756.

Huang S., Frey F. A., Blichert-Toft J., Fodor R. V., Bauer G. R. and Xu G. (2005b) Enriched components in the Hawaiian plume: evidence from Kahoolawe Volcano, Hawaii. *Geochem. Geophys. Geosyst.* **6**, Q11006. http://dx.doi.org/10.1029/2005GC001012.

Huang S., Hall P. S. and Jackson M. G. (2011) Geochemical zoning of volcanic chains associated with Pacific hotspots. *Nat. Geosci.* **4**, 874–878. http://dx.doi.org/10.1038/NGEO1263.

Ireland T. J., Arevalo, Jr., R., Walker R. J. and McDonough W. F. (2009) Tungsten in Hawaiian picrites: a compositional model for the sources of Hawaiian lavas. *Geochim. Cosmochim. Acta* **73**, 4517–4530. http://dx.doi.org/10.1016/j.gca.2009.04.016.

Kamber B. S. and Collerson K. D. (2000) Zr/Nb systematics of ocean island basalts reassessed – the case for binary mixing. *J. Petrol.* **41**, 1007–1021.

Kennedy A. K., Kwon S. T., Frey F. A. and West H. B. (1991) The isotopic composition of postshield lavas from Mauna Kea Volcano, Hawaii. *Earth Planet. Sci. Lett.* **103**, 339–353.

Kurz M. D., Curtice J., Lott, III, D. E. and Solow A. (2004) Rapid helium isotopic variability in Mauna Kea shield lavas from the Hawaiian Scientific Drilling Project. *Geochem. Geophys. Geosyst.* **5**, Q04G14. http://dx.doi.org/10.1029/2002GC000439.

Langmuir C., Klein E. and Plank T. (1992) Petrological systematics of mid-ocean ridge basalts: constraints on melt generation beneath ocean ridges. *AGU Monogr.* **71**, 183–280.

Lindstrom M. M. and Haskin L. A. (1981) Compositional inhomogeneities in a single Icelandic tholeiite flow. *Geochim. Cosmochim. Acta* **45**, 15–31.

Lipman P. W., Rhodes J. M. and Dalrymple G. B. (1990) The Ninole Basalt – implications for the structural evolution of Mauna Loa volcano, Hawaii. *Bull. Volcanol.* **53**, 1–19.

Marske J. P., Pietruszka A. J., Weis D., Garcia M. O. and Rhodes J. M. (2007) Rapid passage of a small-scale mantle heterogeneity through the melting regions of Kilauea and Mauna Loa Volcanoes. *Earth Planet. Sci. Lett.* **259**, 34–50.

Marske J. P., Garcia M. O., Pietruszka A. J., Rhodes J. M. and Norman M. D. (2008) Geochemical variations during Kilauea's Pu'u O'o eruption reveal a fine-scale mixture of mantle heterogeneities within the Hawaiian plume. *J. Petrol.* **49**, 1297–1318. http://dx.doi.org/10.1093/petrology/egn025.

Nobre Silva I. G., Weis D. and Scoates J. S. (2013) Isotopic systematics of the early Mauna Kea shield phase and insight into the deep mantle beneath the Pacific Ocean. *Geophys. Geosyst.* **14**, 659–676. http://dx.doi.org/10.1002/ggge.20047.

Norman M. D., Leeman W. P., Blanchard D. P., Fitton J. G. and James D. (1989) Comparison of major and trace element analyses by ICP, XRF, INAA and ID methods. *Geostand. Newslett.* **13**(2), 283–290.

Pearce J. A. (1996) User's guide to basalt discrimination diagrams in trace element geochemistry of volcanic rocks: applications for massive sulphide exploration. In *Geological Association of Canada* (ed. D. A. Wyman). pp. 79–113.

Pietruszka A. J. and Garcia M. O. (1999) A rapid fluctuation in the mantle source and melting history of Kilauea Volcano inferred from the geochemistry of its historical summit lavas (1790–1982). *J. Petrol.* **40**, 1321–1342.

Pietruszka A. J., Norman M. D., Garcia M. O., Marske J. P. and Burns D. H. (2013) Chemical heterogeneity in the Hawaiian mantle plume from the alteration and dehydration of recycled oceanic crust. *Earth Planet. Sci. Lett.* **361**, 298–309. http://dx.doi.org/10.1016/j.epsl.2012.10.030.

Putirka K., Ryerson F. J., Perfit M. and Ridley W. I. (2011) Mineralogy and composition of the oceanic mantle. *J. Petrol.* **52**, 279–313.

Qin L., Dauphas N., Janney P. E. and Wadhwa M. (2007) Analytical developments for high-precision measurements of W isotopes in iron meteorites. *Anal. Chem.* **79**, 3148–3154.

Révillon S., Teagle D. A. H., Boulvais P., Shafer J. and Neal C. R. (2007) Geochemical fluxes related to alteration of a subaerially exposed seamount: Nintoku seamount, ODP Leg 197, Site 1205. *Geochem. Geophys. Geosyst.* **8**, Q02014. http://dx.doi.org/10.1029/2006GC001400.

Rhodes J. M. (1983) Homogeneity of Lava Flows: chemical data for historical Mauna Loa eruptions. *J. Geophys. Res.* **88**, A869–A879.

Rhodes J. M. (1984) Geochemistry of the 1984 Mauna Loa eruption: implications for magma storage and supply. *J. Geophys. Res.* **93**, 4453–4466.

Rhodes J. M. (1996) Geochemical stratigraphy of lava flows sampled by the Hawaii Scientific Drilling Project. *J. Geophys. Res.* **101**, 11729–11746.

Rhodes J. M. and Vollinger M. J. (2004) Composition of basaltic lavas sampled by phase-2 of the Hawaii Scientific Drilling Project: geochemical stratigraphy and magma types. *Geochem.*

Geophys. Geosyst. **5**, Q03G13. http://dx.doi.org/10.1029/2002GC000434.

Rhodes J. M., Huang S., Frey F. A., Pringle M. and Xu G. (2012) Compositional diversity of Mauna Kea shield lavas recovered by the Hawaii Scientific Drilling Project: inferences on source lithology, magma supply, and the role of multiple volcanoes. *Geochem. Geophys. Geosyst.* **13**(3), Q03014. http://dx.doi.org/10.1029/2011GC003812.

Roden M. F., Frey F. A. and Clague D. A. (1984) Geochemistry of tholeiitic and alkalic lavas from the Koolau Range, Oahu, Hawaii: implications for Hawaiian volcanism. *Earth Planet. Sci. Lett.* **69**, 141–158.

Saal A. E., Kurz M. D., Hart S. R., Blusztajn J. S., Blichert-Toft J., Liang Y. and Geist D. J. (2007) The role of lithospheric gabbros on the composition of Galapagos lavas. *Earth Planet. Sci. Lett.* **257**, 391–406. http://dx.doi.org/10.1016/j.epsl.2007.02.040.

Schramm B., Devey C. W., Gillis K. M. and Lackschewitz K. (2005) Quantitative assessment of chemical and mineralogical changes due to progressive low-temperature alteration of East Pacific Rise basalts from 0 to 9 Ma. *Chem. Geol.* **218**, 281–313.

Seaman C., Sherman S. B., Garcia M. O., Baker M. B., Balta B. and Stolper E. (2004) Volatiles in glasses from the HSDP2 drill core. *Geochem. Geophys. Geosyst.* **5**, Q09G16. http://dx.doi.org/10.1029/2003GC000596.

Sertek J. P., Andrade S. and Ulbrich H. H. (2015) An evaluation of the effects of primary and cross-contamination during the preparation of rock powders for chemical determinations. *Geostand. Geoanal. Res.*. http://dx.doi.org/10.1111/j.1751-908X.2014.00324.x.

Seyfried, Jr, W. E. and Bischoff J. L. (1979) Low temperature basalt alteration by seawater: an experimental study at 70 °C and 150 °C. *Geochim. Cosmochim. Acta.* **43**, 1937–1947.

Sharp W. D. and Renne P. R. (2005) The $^{40}Ar/^{39}Ar$ dating of core recovered by the Hawaii Scientific Drilling Project (phase 2), Hilo, Hawaii. *Geochem. Geophys. Geosyst.* **6**, Q04G17. http://dx.doi.org/10.1029/2004GC000846.

Sobolev A. V., Hofmann A. W. and Nikogosian I. K. (2000) Recycled oceanic crust observed in ghost plagioclase within the source of Mauna Loa lavas. *Nature* **404**, 986–990.

Staudigel H., Gillis K. and Duncan R. (1986) K/Ar and Rb/Sr ages of celadonites from the Troodos ophiolite, Cyprus. *Geology* **14**, 72–75.

Staudigel H., Plank T., While B. and Schmincke H.-U. (1996) Geochemical fluxes during seafloor alteration of the basaltic upper oceanic crust: DSDP Sites 417 and 418. In *Subduction Top to Bottom*, vol. 96 (ed. G. E. Bebout et al.). AGU, Washington, D.C., pp. 19–38.

Stolper E. M., DePaolo D. J. and Thomas D. M. (1996) Introduction to special section; Hawaii Scientific Drilling Project. *J. Geophys. Res.* **101**, 11593–11598.

Stolper E. M., Sherman S., Garcia M., Baker M. and Seaman C. (2004) Glass in the submarine section of the HSDP2 drill core, Hilo, Hawaii. *Geochem. Geophys. Geosyst.* **5**, Q07G15. http://dx.doi.org/10.1029/2003GC000553.

Thompson G. (1984) Basalt-seawater interaction. In *Hydrothermal Processes at Seafloor Spreading Centers* (eds. P. A. Rona, K. Bostrom, L. Laubier and K. L. Smith). Plenum, New York, pp. 225–278.

Walton A. W. and Schiffman P. (2003) Alteration of hyaloclastites in the HSDP 2 Phase 1 Drill Core. 1. Description and paragenesis. *Geochem. Geophys. Geosyst.* **4**, 8709. http://dx.doi.org/10.1029/2002GC00368.

Walton A. W., Schiffman P. and Macpherson G. L. (2005) Alteration of hyaloclastites in the HSDP 2 Phase 1 Drill Core: 2. Mass balance of the conversion of sideromelane to palagonite and chabazite. *Geochem. Geophys. Geosyst.* **6**, Q09G19. http://dx.doi.org/10.1029/2004GC000903.

Weinstein J. P., Fodor R. V. and Bauer G. R. (2004) Koolau shield basalt as xenoliths entrained during rejuvenated-stage eruption: perspectives on magma mixing. *Bull. Volcanol.* **66**, 182–199. http://dx.doi.org/10.1007/s00445-003-0302-1.

Weis D., Kieffer B., Maerschalk C., Pretorium W. and Barling J. (2005) High-precision Pb–Sr–Nd–Hf isotopic characterization of USGS BHVO-1 and BHVO-2 reference materials. *Geochem. Geophys. Geosyst.* **6**, Q02002. http://dx.doi.org/10.1029/2004GC000852.

Weis D., Garcia M. O., Rhodes J. M., Jellinek M. and Scoates J. S. (2011) Role of the deep mantle in generating the compositional asymmetry of the Hawaiian mantle plume. *Nat. Geosci.* **4**, 831–838.

Yang H.-J., Frey F. A., Rhodes J. M. and Garcia M. O. (1996) Evolution of Mauna Kea volcano: inferences from lava compositions recovered in the Hawaii Scientific Drilling Project. *J. Geophys. Res.* **101**, 11747–11767.

Associate editor: Rosemary Hickey-Vargas